Multiple feature-enhanced synthetic aperture radar imaging

Sadegh Samadi [a], Müjdat Çetin [b], Mohammad Ali Masnadi-Shirazi [a]

[a]Dept. of Electrical Engineering, Shiraz University, Shiraz, Iran ,
[b]Sabancı University, İstanbul, Turkey

ABSTRACT

Non-quadratic regularization based image formation is a recently proposed framework for feature-enhanced radar imaging. Specific image formation techniques in this framework have so far focused on enhancing one type of feature, such as strong point scatterers, or smooth regions. However, many scenes contain a number of such features. We develop an image formation technique that simultaneously enhances multiple types of features by posing the problem as one of sparse signal representation based on overcomplete dictionaries. Due to the complex-valued nature of the reflectivities in SAR, our new approach is designed to sparsely represent the magnitude of the complex-valued scattered field in terms of multiple features, which turns the image reconstruction problem into a joint optimization problem over the representation of the magnitude and the phase of the underlying field reflectivities. We formulate the mathematical framework needed for this method and propose an iterative solution for the corresponding joint optimization problem. We demonstrate the effectiveness of this approach on various SAR images.

Keywords: synthetic aperture radar, multiple feature enhancement, sparse signal representation, overcomplete dictionary, image reconstruction, complex valued imaging.

1. INTRODUCTION

Synthetic Aperture Radar (SAR) is an active microwave sensor, with its own illumination, which is capable of producing high-resolution images of the earth's surface at any time. With day and night capability and all weather operation, SAR is one of the most promising remote sensing modalities. SAR uses a sensor carried on an airborne or spaceborne platform, transmitting microwave pulses towards an area of interest on the ground, and receives the reflected signal. This signal first undergoes some pre-processing, involving demodulation. The SAR image formation problem is the problem of reconstruction of a spatial reflectivity distribution of the scene from the pre-processed SAR returns. In order to visualize or distinguish targets in a two dimensional scene, SAR coherently processes multiple pulses to synthesize the effect of a large antenna.

There are two basic modes for a SAR system: stripmap-mode, and spotlight-mode. In stripmap-mode SAR, the antenna pointing direction is fixed, so that the antenna beam sweeps a strip along the ground and a contiguous image is formed. In spotlight-mode SAR, the antenna is steered gradually backwards to continuously illuminate an area of interest on the ground. Although ideas presented in this paper are not limited to a specific mode, here we focus on spotlight-mode SAR. The conventional approach for spotlight-mode SAR image formation is the polar format algorithm (PFA) [1], which is an explicit way to solve the SAR inverse problem, using inverse operators. This method has no explicit mechanism to counter any imperfection (including e.g. noise) in the data, and also suffers from important shortcomings, such as resolution limitation to system bandwidth, speckle, and sidelobe artifacts.

Non-quadratic regularization based image formation is a recently proposed framework for feature-enhanced radar imaging [2,3]. This framework offers a number of advantages over conventional imaging including superresolution; robustness to uncertain or limited data; and enhanced image quality in non-conventional data collection scenarios such as sparse aperture sensing. Specific image formation techniques in this framework have so far focused on enhancing one type of feature in the imaged scene, such as strong point scatterers, or regions with smoothly varying reflectivities. However, many scenes contain, and hence require joint enhancement of, a number of such features. In this paper we develop an image formation technique that simultaneously enhances multiple types of features in the scene. By viewing the image formation problem as a sparse signal representation problem with overcomplete dictionaries, this is achieved by using appropriate dictionaries that combine multiple types of features. We formulate the mathematical framework

needed for this method and solve the corresponding optimization problems. Section 2 provides the details of our mathematical framework as well as our solution to the optimization problems encountered in this framework. In section 3 we present our experimental results on various SAR images to demonstrate the effectiveness of our approach.

2. MULTIPLE FEATURE ENHANCED SAR IMAGING FRAMEWORK

In this section we present our mathematical framework for multiple feature enhanced SAR imaging. As we explained, recent techniques such as nonquadratic regularization[2,3] have mostly focused on enhancement of one type of feature in the process of image formation. Improvements achieved by these methods are the result of using prior information about the scene of interest. This information is incorporated by putting some penalties on the image to be reconstructed from the sampled received data. When the scene is believed to contain multiple types of features (e.g. isolated scatterers, and spatially distributed objects), then the approach in[2,3] appears to suggest adding terms corresponding to each type of feature into the overall cost function to be optimized for imaging. However, this may result in a potentially undesired effect, as multiple and potentially inconsistent constraints could be imposed over the same spatial region. Furthermore, until now, only a very limited set of features have been used in feature-enhanced SAR imaging.

Sparse signal representation has successfully been used for solving inverse problems in a variety of applications. Here we propose a new approach for SAR imaging based on sparse signal representation to overcome the shortcomings mentioned above. Sparse signal representation has many capabilities such as superresolution and feature enhancement in various reconstruction and recognition tasks; however, it has mostly been used in real valued problems. Due to the complex-valued and potentially random phase nature of the reflectivities in SAR, our new approach is designed to sparsely represent the magnitude of the complex-valued scattered field in terms of multiple features, which turns the image reconstruction problem into a joint optimization problem over the representation of the magnitude and the phase of the underlying field reflectivities.

2.1 Observation model

It is shown in[2] that the spotlight-mode SAR system model can be considered as:

$$y = Hf + n \tag{1}$$

where y is the sampled range profile, f is the unknown scene or object reflectivity image, and n is noise; all are complex and column-reordered as vectors. H represents a complex-valued discrete SAR projection operator.

This model is also valid for phase history data by proper definition of the discrete observation kernel H. We can also use this model when y is a conventionally reconstructed image, by letting H be a matrix each row of which contains a spatially shifted version of the corresponding point spread function (PSF) stacked as a row vector [4]. If PSF information is available, this case is attractive from the computational viewpoint because of its convolutional form.

2.2 Sparse representation framework for multiple feature enhanced SAR imaging

In this part we develop our sparse representation algorithm that effectively deals with the complex-valued nature of the SAR signal and can be used for multiple feature enhanced SAR image formation. For simplicity, let us first assume that we are interested in two features to be enhanced simultaneously in the process of SAR image formation. However, we will see that there is no limitation on the number of features in this method and we can easily extend it to any number of features.

Although the unknown scene f in our observation model is complex-valued, in most applications we are interested in features of its magnitude. So we can consider that:

$$|f| = \Phi_1\alpha_1 + \Phi_2\alpha_2 \tag{2}$$

where Φ_1 and Φ_2 are appropriate dictionaries for our application that can sparsely represent the scene in terms of the features of interest, and α_1 and α_2 are vectors of representation coefficients. For any complex-valued vector like f we can write $f = P|f|$, where $P = diag\{e^{j\phi_i}\}$, and ϕ_i's are the unknown phases of each image vector element f_i. So we can rewrite our observation model as:

$$y = Hf + n = HP|f| + n = HP\Phi_1\alpha_1 + HP\Phi_2\alpha_2 + n \tag{3}$$

If we knew *P* (or the phases of the elements of the unknown image vector), using an atomic decomposition technique such as an extension of basis pursuit denoising [5], we could find an estimate of α_1 and α_2 , and hence the image of the unknown scene itself:

$$\{\hat{\alpha}_1, \hat{\alpha}_2\} = \arg \min_{\alpha_1, \alpha_2} \|y - H P \Phi_1 \alpha_1 - H P \Phi_2 \alpha_2\|_2^2 + \lambda \|\alpha_1\|_p^p + \lambda \|\alpha_2\|_p^p \quad (4)$$

Where $\|\cdot\|_p$ denotes the ℓ_p -norm, and λ is a positive real scalar parameter. Note that the ℓ_2 -norm term in (4) is related to the assumption that noise is zero mean white Gaussian noise. Also note that the perfect sparsity condition term is ℓ_0 -norm that leads to a combinational, hard to solve problem, however it is shown [6-9] that fields that admit a sparse enough representation, the ℓ_p -norm with $p \leq 1$, that we use, also leads to the sparsest of all representations under certain conditions.

However, the problem to solve the optimization problem in (4) is that we don't know the phase terms of the image vector elements and hence *P*. We propose the following joint optimization approach to overcome this problem:

a. We start with an initial estimate for *f* that could be a conventional reconstruction of *f*. Using this *f*, we produce an initial estimate of the image phase matrix *P*.

b. Using this estimate of *P*, we can solve the optimization problem in (4) and find a new estimate for α_1 and α_2.

c. Using the new estimates of α_1 and α_2 we can produce our new estimate for $|f|$. We should now find a new estimate for the phase matrix *P*. To do this we rewrite our observation model as:

$$y = H P |f| + n = H B \beta + n \quad (5)$$

where $B = diag\{|f_i|\}$ and β is vector of unknown phase terms, hence a vector containing the diagonal elements of *P*. An estimate of β can be found as follows:

$$\hat{\beta} = \arg \min_{\beta} \|y - H B \beta\|_2^2 \quad subject\ to \quad |\beta_i| = 1, \forall i \quad (6)$$

We replace the constrained optimization problem in (6), with the following unconstrained problem that incorporates a penalty term on the magnitudes of β_i'*s* :

$$\hat{\beta} = \arg \min_{\beta} \|y - H B \beta\|_2^2 + \lambda' \sum_{i=1}^{N} (|\beta_i|^q - 1)^2$$

$$= \arg \min_{\beta} \|y - H B \beta\|_2^2 + \lambda' \|\beta\|_{2q}^{2q} - 2\lambda' \|\beta\|_q^q \quad (7)$$

Solving this optimization problem will give us a new estimate for the phase vector β and so the matrix $P = diag\{\beta\}$.

d. We are now back to step **(*b*)** and repeat this loop until the algorithm converges to its final solution.

2.3 Solving the joint optimization problems

Let us call the multivariate cost function of the optimization problem (4) $J(\alpha_1,\alpha_2)$, and use the smooth approximation $\|\alpha\|_p^p \approx \sum_{i=1}^{M} (|\alpha_i|^2 + \varepsilon)^{p/2}$, where ε is a small positive constant, to avoid the nondifferentiability problem of the ℓ_p -norm around the origin. The partial gradient of $J(\alpha_1,\alpha_2)$ with respect to α_1 and α_2 will be:

$$\nabla_{\alpha_1} J(\alpha_1, \alpha_2) = G_1(\alpha_1)\, \alpha_1 - 2 (H P \Phi_1)^H (y - H P \Phi_2 \alpha_2) \quad (8)$$

$$\nabla_{\alpha_2} J(\alpha_1, \alpha_2) = G_2(\alpha_2)\, \alpha_2 - 2 (H P \Phi_2)^H (y - H P \Phi_1 \alpha_1) \quad (9)$$

where

$$G_1(\alpha_1) = 2(H P \Phi_1)^H (H P \Phi_1) + \lambda\, p\, \Lambda(\alpha_1) \tag{10}$$

$$G_2(\alpha_2) = 2(H P \Phi_2)^H (H P \Phi_2) + \lambda\, p\, \Lambda(\alpha_2) \tag{11}$$

and the $\Lambda(\cdot)$ function is:

$$\Lambda(\alpha) = diag\left\{ \frac{1}{(|\alpha_i|^2 + \varepsilon)^{1-p/2}} \right\} \tag{12}$$

in which, α_i's are the elements of the vector α. By setting the gradient terms in (8) and (9) to zero, we reach the following results:

$$\begin{aligned}
&\nabla_{\alpha_1} J(\alpha_1, \alpha_2) = 0 \Rightarrow\ G_1(\alpha_1)\ \alpha_1 + 2(H P \Phi_1)^H (H P \Phi_2)\ \ \alpha_2 = 2(H P \Phi_1)^H\, y \\
&\nabla_{\alpha_2} J(\alpha_1, \alpha_2) = 0 \Rightarrow\ G_2(\alpha_2)\ \alpha_2 + 2(H P \Phi_2)^H (H P \Phi_1)\ \ \alpha_1 = 2(H P \Phi_2)^H\, y \\
&\Rightarrow \begin{bmatrix} G_1(\alpha_1) & 2(H P \Phi_1)^H (H P \Phi_2) \\ 2(H P \Phi_2)^H (H P \Phi_1) & G_2(\alpha_2) \end{bmatrix} \begin{bmatrix} \alpha_1 \\ \alpha_2 \end{bmatrix} = \begin{bmatrix} 2(H P \Phi_1)^H\, y \\ 2(H P \Phi_2)^H\, y \end{bmatrix} \\
&\Rightarrow \widetilde{G}(\widetilde{\alpha})\ \widetilde{\alpha} = \widetilde{y}
\end{aligned} \tag{13}$$

in which $\widetilde{\alpha} = \begin{bmatrix} \alpha_1 \\ \alpha_2 \end{bmatrix}$. Note that in (13) $\widetilde{G}$ is a function of $\widetilde{\alpha}$ so it doesn't yield a closed form solution for $\widetilde{\alpha}$ in general, so numerical optimization techniques should be used. It has been shown [2,10] that standard methods such as Newton's method or quasi-Newton's method with a conventional Hessian update scheme, perform poorly in nonquadratic problems. Using the idea in [2], we use here a quasi-Newton's method with a Hessian update scheme that is matched to the structure of our problem.

Rewriting the cost function $J(\alpha_1, \alpha_2)$ in terms of $\widetilde{\alpha}$ and taking its gradient, we obtain:

$$\nabla J(\widetilde{\alpha}) = \widetilde{G}(\widetilde{\alpha})\ \widetilde{\alpha} - \widetilde{y} \tag{14}$$

We use $\widetilde{G}(\widetilde{\alpha})$ as an approximation to the Hessian and use it in the following quasi-Newton's iterative algorithm:

$$\hat{\widetilde{\alpha}}^{(n+1)} = \hat{\widetilde{\alpha}}^{(n)} - \gamma [\widetilde{G}(\hat{\widetilde{\alpha}}^{(n)})]^{-1} \nabla J(\hat{\widetilde{\alpha}}^{(n)}) \tag{15}$$

After substituting (14) in (15) and rearranging, we obtain the following iterative algorithm:

$$\widetilde{G}(\hat{\widetilde{\alpha}}^{(n)})\ \hat{\widetilde{\alpha}}^{(n+1)} = (1-\gamma)\ \widetilde{G}(\hat{\widetilde{\alpha}}^{(n)}) + \gamma\, \widetilde{y} \tag{16}$$

The algorithm can be started from an initial estimate of $\widetilde{\alpha}$ and run until convergence occurs. Note that $\widetilde{G}(\hat{\widetilde{\alpha}}^{(n)})$ in our problem is sparse, Hermitian symmetric and positive semidefinite so the set of linear equations in (16) for finding $\hat{\widetilde{\alpha}}^{(n+1)}$ can itself be solved efficiently using iterative approaches such as Conjugate Gradient (CG), which we use in our method.

In a similar way to the above discussion we can obtain the following iterative algorithm for solving the optimization problem in (7):

$$G(\hat{\beta}^{(n)})\ \hat{\beta}^{(n+1)} = (1-\gamma)\ G(\hat{\beta}^{(n)}) + 2\gamma (H B)^H y \tag{17}$$

where

$$G(\beta) = 2(H B)^H (H B) + 2\lambda' q\, \Lambda_1(\beta) - 2\lambda' q\, \Lambda_2(\beta) \tag{18}$$

$$\Lambda_1(\beta) = diag\left\{\frac{1}{(|\beta_i|^2 + \varepsilon)^{1-q}}\right\}$$

$$\Lambda_2(\beta) = diag\left\{\frac{1}{(|\beta_i|^2 + \varepsilon)^{1-q/2}}\right\} \tag{19}$$

2.4 Extension to any number of features and arbitrary overcomplete dictionaries

Let $\widetilde{\Phi}$ be an overcomplete dictionary containing Φ_1 and Φ_2, i.e. $\widetilde{\Phi} = [\Phi_1 \quad \Phi_2]$, and as we defined before, let $\tilde{\alpha}$ be equal to $\begin{bmatrix}\alpha_1 \\ \alpha_2\end{bmatrix}$, so that we can write:

$$|f| = \widetilde{\Phi}\ \tilde{\alpha} \tag{20}$$

We can now rewrite (3) as:

$$y = H\,f + n = H\,P|f| + n = H\,P\widetilde{\Phi}\ \ \tilde{\alpha}\ + n \tag{21}$$

and the optimization problem (4) becomes:

$$\hat{\tilde{\alpha}} = \arg\ \min_{\tilde{\alpha}}\ \left\|y - H\,P\widetilde{\Phi}\,\tilde{\alpha}\right\|_2^2 + \lambda\|\tilde{\alpha}\|_p^p \tag{22}$$

Gradient of the cost function in (24) with respect to $\tilde{\alpha}$ is:

$$\nabla J(\tilde{\alpha}) = \widetilde{G}'(\tilde{\alpha})\ \tilde{\alpha} - 2(H\,P\widetilde{\Phi})^H y \tag{23}$$

where

$$\widetilde{G}'(\tilde{\alpha}) = 2(H\,P\widetilde{\Phi})^H (H\,P\widetilde{\Phi}) + \lambda\, p\,\Lambda(\tilde{\alpha}) \tag{24}$$

It can be easily shown that $\widetilde{G}'(\tilde{\alpha})$ in (24) is exactly equal to $\widetilde{G}(\tilde{\alpha})$ in (13), and also $\tilde{y} = 2(H\,P\widetilde{\Phi})^H y$. So the optimization problem in (24) becomes exactly equivalent to (4) and the solution obtained in (16) is also valid for it. So in general, we can easily extend our approach to incorporate any number of features that we want to be enhanced in the process of SAR image formation, by considering an overcomplete dictionary $\widetilde{\Phi} = [\Phi_1 \quad \Phi_2 \quad \Phi_3 \quad \ldots]$, in which each subdictionary sparsely represents one of the features of interest, and then use the same iterative algorithm in (16) by using the general form of the matrix $\widetilde{G}'(\tilde{\alpha})$ given in (24).

It is apparent that any dictionary $\widetilde{\Phi}$ that sparsely represents multiple features, such as multiresolution dictionaries (e.g. wavelets), can be used in this framework and its effectiveness will be dependent on how well it can sparsely represents the multiple features of interest.

2.5 Dictionary selection

Selection of the proper dictionary $\widetilde{\Phi}$ is an important part of this method. This dictionary should sparsely represent the magnitude of the complex-valued image which contains multiple features of interest, and so it depends on the application and the type of objects or features of interest in our image.

2.5.1 Overcomplete shape-based (SB) dictionaries

If our scene can be represented as a combination of some limited simple shapes such as points, lines, and squares of different sizes, and so on, then a trivial powerful dictionary can be constructed by gathering all possible positions of these fundamental elements in an overcomplete dictionary. This type of dictionary is very powerful to show capabilities of the framework for synthetic or simple real scenes. For example if we are interested in point scatterers along with smooth regions with simple shapes in a SAR image, use of this type of dictionary produces excellent results. Although

this type of dictionary has interesting properties, in large scale problems it can lead to computational difficulties because of the required large number of dictionary atoms. So we need to find more efficient dictionaries for practical applications. The use of such an overcomplete dictionary is demonstrated in Section 3 on some synthetic scenes.

2.5.2 Point and region-based (PR) dictionary

Since the case of point-like targets and smooth regions are two interesting features in SAR images and the previously introduced dictionary is not computationally efficient for it, we propose this simple dictionary which is much more efficient. This dictionary is a combination of two subdictionaries. The point subdictionary is a dictionary of isolated point scatterers at all possible positions. Considering our formulation in the previous sections, for a SAR image of size N×N, the size of this subdictionary is $N^2 \times N^2$. More specifically it is an identity matrix of the above size. For region-based subdictionary we propose to use an inverse of discrete two-dimensional gradient operator. It is also an $N^2 \times N^2$ dictionary. To better understand that how this dictionary works and provide a flavor of it we present a one-dimensional region dictionary, which is equivalently the inverse of a discrete derivative operator. For a 1-D signal of length 4, this dictionary is:

$$\Phi = \begin{bmatrix} 1 & 1 & 1 & 1 \\ 0 & 1 & 1 & 1 \\ 0 & 0 & 1 & 1 \\ 0 & 0 & 0 & 1 \end{bmatrix}$$

It is apparent that this form of dictionary could be appropriate for sparsely representing smooth 1-D signals.

2.5.3 Wavelet dictionary

Standard multiresolution dictionaries, such as those based on wavelets are one of the effective options that can be used in our framework. Previous works have established that wavelet transform can sparsely represent natural scene images [11,12]. The application of wavelet transforms to image compression leads to impressive results over other representations, so this dictionary has the ability to sparsely represent complicated images containing numerous features.

2.5.4 Other dictionaries

Depending on our application, we may need to use other dictionaries with properties matched to that application. For example curvelet transform enables directional analysis of an image in different scales, so it is well suited for enhancing features like edges and smooth curves in an image. If we have textures with periodic patterns in our magnitude image then one appropriate dictionary to sparsely represent these patterns could be based on the discrete cosine transform (DCT).

There exist many other popular dictionaries, which we don't mention here for the sake of brevity. We should just point out that any such dictionary could be used in our framework, if it is appropriate for the particular application of interest.

3. EXPERIMENTAL RESULTS

We present here our results of experiments with various synthetic and real SAR scenes to demonstrate the effectiveness of our method. We compare our results with conventional and nonquadratic regularization methods to show the improvements achieved. We also show results of our method with different dictionaries to show the effect of dictionary selection and the capability of the proposed framework to work with any appropriate dictionary.

3.1 Parameter selection and initialization of the algorithm

We have used the conventional polar format reconstruction as an initial estimate for f ,both in our method and in the nonquadratic regularization method, and so we can find an initial estimate for both $\widetilde{\alpha}$ and β. In the iterative algorithms in (16) and (17) we have used a fixed step size of γ=1. Of course, to modify the convergence properties of the algorithm, when it is necessary, we can use a smaller or even a variable step size. The smoothing parameter ε, in the definition of the approximate ℓ_p -norm, is set to 10^{-5} , which is small enough to not affect on computation results.

For synthetic image experiments we have used parameters of a spotlight mode SAR of 10 GHz center frequency and 0.375 m range and cross range resolution.

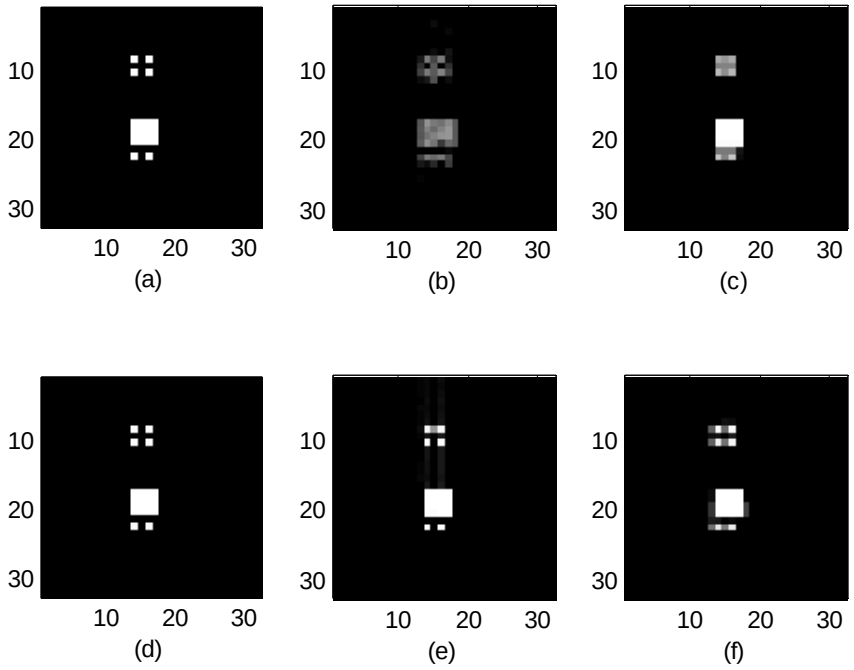

Fig. 1. Synthetic scene reconstruction (a) synthetic scene (b) conventional reconstruction (c) point-region-enhanced nonquadratic regularization (d)-(f) sparse representation based reconstructions : (d) SB dictionary (e) PR dictionary (f) wavelet dictionary.

3.2 Synthetic scene reconstruction

To demonstrate the multiple feature enhancement capability of our framework, in the first experiment, we use a synthetic scene composed of point scatterers and a smooth distributed region as shown in Fig. 1(a). Our image consists of 32×32 complex-valued pixels, and we show only the magnitude field in Fig. 1(a). Phase is randomly distributed with a uniform density function in $[-\pi,\pi]$.

The conventional image reconstruction based on the polar format algorithm (PFA) is shown in Fig. 1(b), and Fig. 1(c) shows the nonquadratic regularization method developed in [1] with penalties for both point and region enhancement. Note that this method cannot enhance both types of features simultaneously in the reconstructed image. As we discussed before, this happens because of applying two contrary penalties on the whole image. Whether the points or the regions are better preserved could be adjusted through the regularization parameters, but this involves a tradeoff.

Fig. 1(d) through Fig. 1(f) show the reconstructed images with our method using different dictionaries described in subsections 2.5.1 through 2.5.3. The shape-based dictionary here, which consists of points as well as squares of various sizes at every possible location of the scene, has an excellent sparse representation for the magnitude of this synthetic image, so the reconstructed image with this dictionary is very close to perfect reconstruction. Note that for better comparison of all results, we haven't shown values below 40 dB of the maximum value of the image.

Point and region-based (PR) dictionary is computationally much more efficient and its result is also very good in comparison to the conventional and nonquadratic regularization-based methods. The multiresolution wavelet dictionary is a much more general dictionary that can be used for unknown complicated scenes. Here we have used the Haar wavelet. Its result, shown in Fig. 1(f), is also good and interesting. If we are interested in special features such as point scatterers, it is also possible to construct an overcomplete dictionary composed of a point dictionary (i.e. spikes) and wavelets. Parameters used in this part are λ=7, $\lambda' = 1$, and p=q=0.6 .

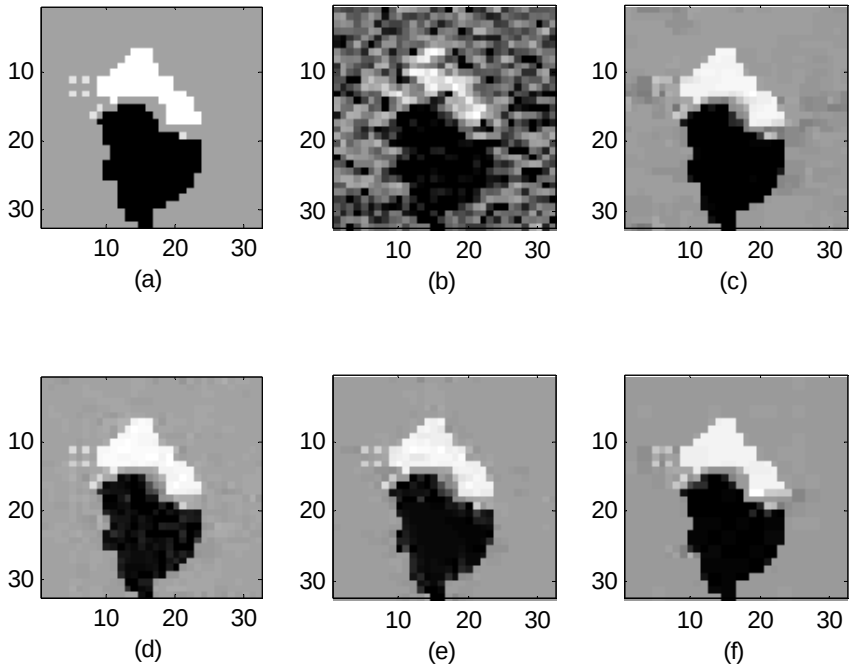

Fig. 2. Synthetic ADTS scene reconstruction (a) synthetic scene (b) conventional reconstruction (c) point-region-enhanced nonquadratic regularization (d)-(f) sparse representation based reconstructions: (d) SB dictionary (e) PR dictionary (f) wavelet dictionary

To be more realistic, in the next experiment we use a synthetic image, constructed from the MIT Lincoln Laboratory Advanced Detection Technology Sensor (ADTS) data set [13] by segmentation techniques, as well as addition of some point scatterers (with random phase) to it, as shown in Fig. 2(a). Conventional and nonquadratic regularization reconstructions are shown in Fig. 2(b) and Fig. 2(c) respectively. We have used the same shape-based dictionary described in the previous experiment. Because of nonzero background and arbitrary distributed regions, the representation of this image is not as sparse as the previous synthetic scene, however the reconstructed image is still good. We can see that for this more realistic scene, wavelet dictionary has an excellent result. Parameters used in this part are λ= 10, p=0.6, $\lambda' = 5$, q=0.6 for the shape-based dictionary result, and q=1 for other results. We have used the Haar wavelet for this experiment too.

3.3 AFRL Backhoe data

We now present our experimental results based on the AFRL Backhoe Data [14], which is a wideband, full polarization, complex-valued backscattered data from a backhoe vehicle (shown in Fig. 3) in free space. In our experiment we use VV polarization data centered at 10 GHz with a 1 GHz bandwidth, with an azimuthal span of 110° (centered at 45°). Fig. 4(a) shows conventional reconstruction of this data. A point enhanced nonquadratic regularization method for this data has been recently presented in [4]. Fig. 4(b) shows the reconstructed image based on this technique. Fig. 4(c) and Fig. 4(d) show the results based on our method using PR and wavelet dictionaries. As we expected, for this complicated scene wavelet dictionary shows a very good result with very little artifacts and arguably with a good tradeoff between resolvability of strong point scatterers and preservation of smooth reflectivity regions.

Parameters which are used in this experiment are λ= 0.2, p=0.3, $\lambda' = 10$, and q=1 for PR dictionary result and λ= 1, p=0.9, $\lambda' = 1$, and q= 0.3 for wavelet dictionary result. We have used the Daubechies 2 (db2) wavelet for this experiment.

Fig. 3. The backhoe vehicle model

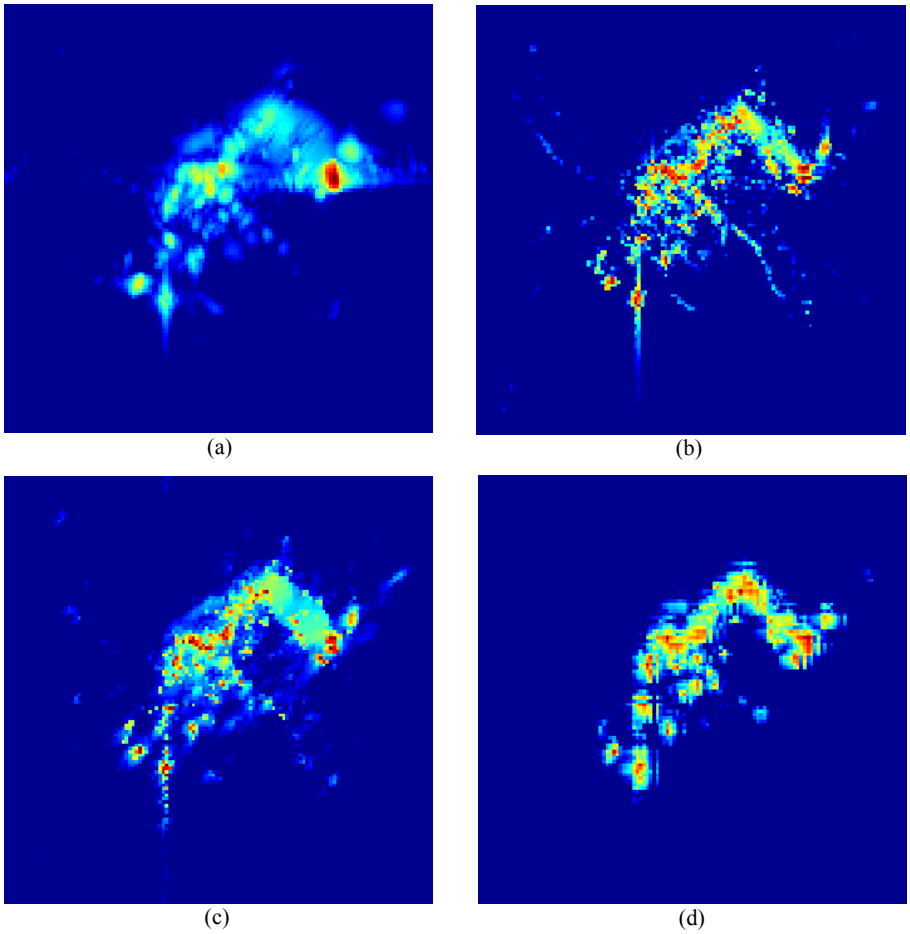

Fig. 4. Results with the AFRL Backhoe data (a) conventional reconstruction (b) point-enhanced nonquadratic regularization (c)-(d) sparse representation based reconstructions : (c) PR dictionary (d) wavelet dictionary

4. CONCLUSIONS

In this paper we have considered the multiple feature enhanced SAR image reconstruction problem. We have proposed an approach based on sparse signal representation using overcomplete dictionaries. Due to the complex-valued nature of the SAR reflectivities, we have designed our approach to sparsely represent the magnitude of the complex-valued scattered field in terms of multiple features. We have formulated the mathematical framework needed for this method and proposed an iterative algorithm to solve the corresponding joint optimization problem over the representation of the magnitude and the phase of the underlying field reflectivities. We have demonstrated the effectiveness of this approach on various SAR images. In addition to multiple feature enhancement, this approach has many other capabilities as by-products including superresolution, robustness to uncertain and limited data, and enhanced image quality in non-conventional data collection scenarios such as sparse aperture sensing, which are known capabilities of the framework used in our approach [15].

ACKNOWLEDGMENTS

This work was partially supported by the Scientific and Technological Research Council of Turkey under Grant 105E090, and by a Turkish Academy of Sciences Distinguished Young Scientist Award.

REFERENCES

[1] Carrara, W. G., Goodman, R. S. and Majewski, R. M., [Spotlight Synthetic Aperture Radar: Signal Processing Algorithms], Artech House, Boston, MA, (1995).

[2] Çetin, M. and Karl, W.C., "Feature-enhanced synthetic aperture radar image formation based on nonquadratic regularization", IEEE Trans. Image Processing 10, 623–631 (2001).

[3] Çetin, M., Karl, W. C., and Willsky, A. S., "Feature-preserving regularization method for complex-valued inverse problems with application to coherent imaging", Optical Engineering 45(1) : 017003, (2006).

[4] Çetin, M. and Moses, R. L., "SAR imaging from partial-aperture data with frequency-band omissions", SPIE Defense and Security Symposium, Algorithms for Synthetic Aperture Radar Imagery XII, E. G. Zelnio and F. D. Garber, Eds., Orlando, Florida, (2005).

[5] Chen, S. S., Donoho, D. L. and Saunders, M. A., "Atomic decomposition by basis pursuit", SIAM J. Sci. Comput., Vol. 20, 33-61 (1998).

[6] Donoho, D. L. and Huo, X., "Uncertainty principles and ideal atomic decomposition", IEEE Trans. Inf. Theory 47(7), 2845–2862 (2001).

[7] Donoho, D. L. and Elad, M., "Maximal sparsity representation via l minimization ", Proc. Nat. Acad. Sci. 100, 2197–2202 (2003).

[8] Elad, M. and Bruckstein, A. "A generalized uncertainty principle and sparse representation in pairs of bases ", IEEE Trans. Inf. Theory 48(9), 2558–2567 (2002).

[9] Gribonval, R. and Nielsen, M., "Some remarks on nonlinear approximation with schauder bases ", East J. Approx. 7(2), 267–285 (2001).

[10] Vogel, C. R. and Oman, M. E., "Iterative methods for total variation denoising", SIAM J. Sci. Comput. 17(1), 227–238 (1996).

[11] Starck, J. L., Elad, M., and Donoho, D. L., "Image decomposition via the combination of sparse representations and a variational Approach", IEEE Trans. Image Processing 14, 1570-1582 (2005).

[12] Donoho, D. L. and Johnstone, I., "Ideal spatial adaptation via wavelet shrinkage", Biometrika 81, 425-455 (1994).

[13] Air Force Research Laboratory, Model Based Vision Laboratory, Sensor Data Management System ADTS, http://www.mbvlab.wpafb.af.mil/public/sdms/datasets/adts/.

[14] Backhoe Data Sample & Visual-D Challenge Problem, Air Force Research Laboratory, Sensor Data Management System, https://www.sdms.afrl.af.mil/main.htm.

[15] Samadi, S., Çetin, M. and Masnadi-Shirazi, M. A., "Sparse signal representation for complex-valued imaging", IEEE 13th Digital Signal Processing Workshop and 5th IEEE Signal Processing Education Workshop, DSP/SPE 2009, (2009).